



ELSEVIER

Available online at www.sciencedirect.com

SCIENCE @ DIRECT®

Journal of Crystal Growth 251 (2003) 532–537

JOURNAL OF
**CRYSTAL
GROWTH**

www.elsevier.com/locate/jcrysgro

Controlled n-type doping of antimonides and arsenides using GaTe

Brian R. Bennett*, R. Magno, N. Papanicolaou

Electronics Science and Technology Division, Naval Research Laboratory, Code 6876, 4555 Overlook Avenue, SW Washington, DC 20375-5347, USA

Abstract

GaTe was used as a dopant source in molecular beam epitaxy to grow n-type AlSb, GaSb, InAs, and GaAs. Carrier density was independent of host material and growth temperature between 350°C and 550°C. Calibrations based upon the binary results were applied to alloys of InAlAsSb for high-frequency transistor applications. Controlled doping of these alloys was achieved at growth temperatures of 350°C and 400°C. Growth of a nominally undoped GaAs layer immediately after use of the GaTe cell indicated no significant memory effects.

© 2002 Elsevier Science B.V. All rights reserved.

PACS: 72.80.Ey; 73.61.Ey; 81.05.Ea

Keywords: A1. Doping; A3. Molecular beam epitaxy; B1. Antimonides; B2. Semiconducting III–V materials; B2. Semiconducting quaternary alloys; B2. Semiconducting gallium compounds

1. Introduction

Antimonide-based compound semiconductors are of interest for a number of novel electronic and optoelectronic devices [1]. For example, field-effect transistors can be fabricated with a high-mobility InAs channel and AlSb barriers. Superlattices consisting of InAs, InGaSb, and AlSb are being explored for infrared detector and laser applications. Most arsenide-based molecular beam epitaxy (MBE) systems use Be and Si as p- and n-type dopants, respectively. Beryllium, a column II element, acts as an acceptor in antimonides as well as arsenides, replacing the group-III

elements. Silicon, a column IV element, is an amphoteric dopant in the III–Vs. It is predominantly a donor in the arsenides, but is an acceptor in GaSb, AlSb, and related alloys [2]. Hence, there is a clear need for an n-type dopant in the antimonides.

Chalcogens such as S, Se, and Te are in column VI of the periodic table and hence logical candidates for n-type dopants in III–V semiconductors. As discussed by Furukawa and Mizuta [3], elemental sources such as Te have a very high vapor pressure and hence are not suitable for MBE. An alternative is to use chalcogenides such as PbSe and GaTe. Wood demonstrated n-type doping of GaAs using PbSe and PbS [4]. Furukawa and Mizuta successfully used GaTe to dope AlGaSb layers n-type in a transistor [3]. Subbanna et al. completed a detailed study of AlSb and GaSb

*Corresponding author. Tel.: +1-202-767-3665; fax: +1-202-767-1165.

E-mail address: brian.bennett@nrl.navy.mil (B.R. Bennett).

doping by PbTe [5]. They achieved controllable carrier concentrations from 10^{16} to 10^{18} cm^{-3} . In this work, we used GaTe to dope binary, ternary, and quaternary III–V semiconductors. We also examined possible problems with cell cross talk and MBE memory effects associated with the use of Te.

2. Experimental procedures and results

Growths were carried out in a Riber 32P solid-source MBE system. It includes conventional effusion cells for In, Ga, Al, Si, Be, and GaTe as well as a valved As cracker and an unvalved Sb cracker. We used stoichiometric Ga_1Te_1 (hereafter referred to as GaTe) from Cerac. Ten to fifteen pieces, each weighing approximately 100 mg, were loaded. After outgassing at 425°C , we obtained higher-than-expected carrier concentrations: $n \sim 10^{18}$ cm^{-3} for GaAs(Te) with $T_{\text{GaTe}} = 350^\circ\text{C}$. Following additional outgassing at 500°C , the carrier densities were at lower levels and reproducible for all semiconductors investigated (this is in agreement with work at M.I.T. Lincoln Laboratories [6]). This is consistent with the evaporation of elemental Te or Ga_2Te_3 during the initial growths and outgassing [3].

Thick (1–5 μm) binary layers of GaAs, GaSb, and AlSb were grown on semi-insulating GaAs substrates at a growth rate of 1.0 monolayers/s (1.0–1.1 $\mu\text{m}/\text{h}$). Carrier densities and mobilities were measured by the Hall/Van der Pauw technique; densities are plotted in Fig. 1. Note that the results are consistent for GaAs, AlSb, and GaSb. The growth temperatures for the GaAs layers were 550 – 600°C , compared to 500°C and 450°C for AlSb and GaSb, respectively. Polaron electrochemical profiling measurements were performed on the GaAs sample with $T_{\text{GaTe}} = 450^\circ\text{C}$ and yielded a relatively uniform concentration of 1.5 – 2.0×10^{17} cm^{-3} , in good agreement with the Hall measurements. We fit the transport data for GaAs, GaSb, AlSb, and InAlAsSb to calculate the activation energy for the GaTe cell: 1.65 eV. This result is smaller than other reported values: 2.1 [7] and 2.6 eV [8]. The other data in Fig. 1 will be discussed later.

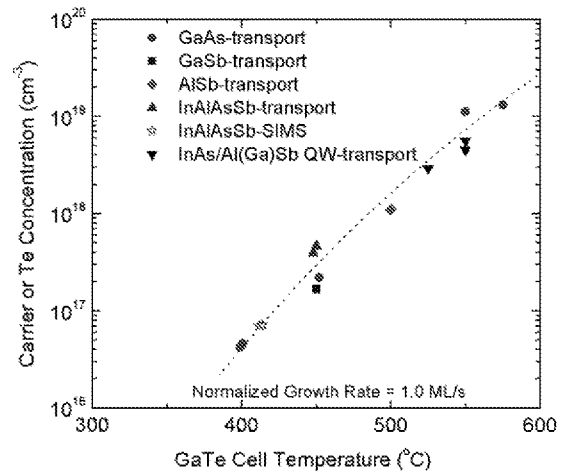


Fig. 1. Electron density or Te concentration versus GaTe cell temperature based upon Hall/van der Pauw measurements of 1–5 μm thick layers, transport measurements of InAs quantum wells, and SIMS measurements of InAlAsSb films. The line is a fit to the single-layer transport data and corresponds to an activation energy of 1.65 eV.

We are currently exploring GaTe doping for two device programs using antimonide-based compound semiconductors. The first is heterojunction bipolar transistors (HBTs) at a lattice constant near 6.2 \AA . Based upon band structure considerations, we selected an npn design with an InGaSb base and InAlAsSb emitter and collector. We demonstrated that despite a predicted miscibility gap, high-quality $\text{In}_{0.52}\text{Al}_{0.48}\text{As}_{0.25}\text{Sb}_{0.75}$ can be grown at temperatures of 350°C and 400°C [9]. Higher growth temperatures resulted in poor photoluminescence and X-ray characteristics. The next step was to demonstrate n-type doping of the InAlAsSb quaternary layers. In some alloys such as AlGaAs, the use of low growth temperatures precludes successful doping. We have found, however, that GaTe dopes the quaternary n-type with carrier densities similar to the binary layers [10].¹ Two data points at a GaTe temperature of

¹ We initially attempted Si doping of these alloys. An earlier report of Ref. [10] indicated n-type doping for Si in InAlAsSb but the alloy compositions were different from what we are using here. Our $\text{In}_{0.52}\text{Al}_{0.48}\text{As}_{0.25}\text{Sb}_{0.75}(\text{Si})$ samples were usually very resistive. Hence, we switched to GaTe doping.

450°C are shown in Fig. 1. The growth temperatures for these two samples were 350°C and 400°C. The carrier concentrations for both samples are approximately $4 \times 10^{17} \text{ cm}^{-3}$.

Diodes consisting of p-InAlAsSb on n-InAlAsSb and p-InGaSb on n-InAlAsSb were grown on GaSb substrates. Secondary ion mass spectroscopy (SIMS) measurements were performed to measure the Te incorporation. SIMS data for the homojunction is shown in Fig. 2. Although a complete SIMS calibration for Te in InAlAsSb has not been performed, the measured results, $\sim 7 \times 10^{16} \text{ cm}^{-3}$, are in good agreement with the transport measurements in Fig. 1. Note that on either side of the $1 \mu\text{m}$ $\text{In}_{0.52}\text{Al}_{0.48}\text{As}_{0.25}\text{Sb}_{0.75}(\text{Te})$ layer, the Te concentration drops to below the detection limit of the SIMS ($< 1 \times 10^{15} \text{ cm}^{-3}$). The Te doping profile is abrupt to within the resolution of these SIMS measurements, $\sim 500 \text{ \AA}$. Similar results were obtained by Subbanna et al. for PbTe doping of AlSb and GaSb [5]. This is an encouraging sign, but HBT layers are typically hundreds of angstroms thick. Hence, we cannot be certain that the Te profiles are suitably abrupt until HBTs are fabricated. We

also note that the Sb and Al profiles are relatively flat throughout the quaternary layers in Fig. 2. This indicates that the alloy composition is stable.

The second device project is to demonstrate high-electron-mobility transistors (HEMTs) with lattice constants of 6.1–6.2 Å. The use of GaTe allows the design of a ‘conventional’ modulation-doped structure with an InAs channel, followed by an AlSb spacer layer, and then an AlSb(Te) layer to supply electrons to the channel. Previous work in this area has included both bulk doping of AlSb with Te [11] as well as delta-doped Te layers in AlSb [12–14]. In Fig. 3a, we show the complete cross-section of heterostructures designed for high-frequency, low-power HEMTs. We have previously published HEMT characteristics of similar structures using an As-soak technique or 12 Å layers of InAs(Si) as the source of electrons [15–17]. Details of the various layers can be found in these references. Room-temperature transport measurements on the heterostructure in Fig. 3a yield a sheet carrier density of $3.1 \times 10^{12} \text{ cm}^{-2}$ and a mobility of $18,000 \text{ cm}^2/\text{Vs}$. The sheet resistivity is $114 \Omega/\text{sq}$.

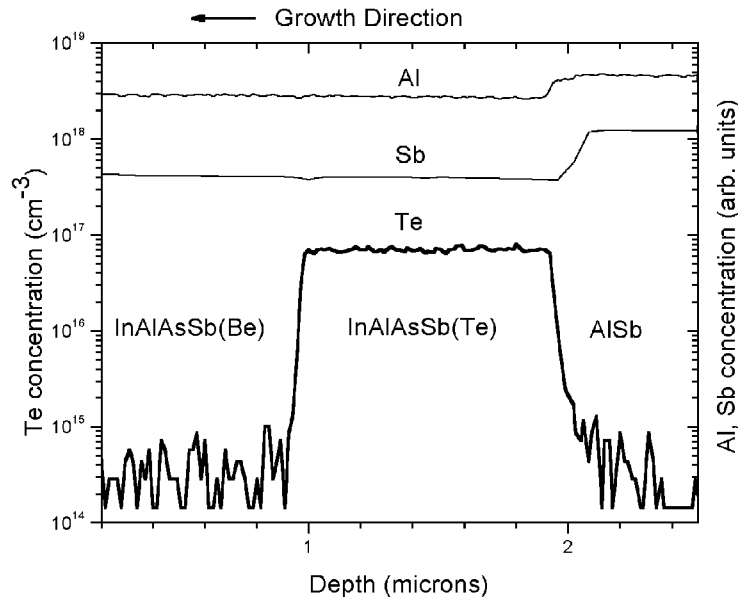


Fig. 2. SIMS profile of Te, Al, and Sb for an InAlAsSb p-n homojunction. Note that the Te concentration drops to instrument-limited background levels outside the $1.0 \mu\text{m}$ doped region.

InAs 20 Å	InAs 20 Å
In _{0.4} Al _{0.6} As 40 Å	In _{0.4} Al _{0.6} As 40 Å
AlSb(Te) 75 Å T _{GaTe} =525°C	AlSb(Te) 35 Å T _{GaTe} =550°C
AlSb 75 Å	AlSb 40 Å
InAs 100 Å	InAs 100 Å
AlSb 30 Å	AlSb 30 Å
InAs 42 Å	InAs 42 Å
AlSb 500 Å	AlSb 500 Å
p-GaSb(Si) 100 Å	p-GaSb(Si) 100 Å
Al _{0.7} Ga _{0.3} Sb 2 μm	Al _{0.7} Ga _{0.3} Sb 2 μm
GaAs	GaAs
SI GaAs(001) substrate	SI GaAs(001) substrate

(a)

(b)

Fig. 3. Layer structures for InAs quantum wells for HEMT applications. The structure in (b) has a Te-doped AlSb layer that is thinner and more heavily doped than the structure in (a). The structure in (b) also has a thinner undoped AlSb spacer layer.

For high-speed operation, small device dimensions are required; we routinely fabricate HEMTs with a gate length of 0.1 μm. As lateral device dimensions are scaled down, it is also important to minimize the vertical dimensions, in particular, the thickness of the material above the channel. For this reason, we modified the structure in Fig. 3a, reducing the AlSb spacer thickness from 75 to 40 Å and decreasing the doped AlSb layer from 75 to 35 Å, as shown in Fig. 3b. To compensate for the thinner doped layer, the GaTe cell temperature was increased by 25°C. The resulting heterostructure sheet carrier density is $2.2 \times 10^{12} \text{ cm}^{-2}$ and the mobility is 22,000 cm²/Vs. If we assume that the contribution of intrinsic carriers is negligible and that all the donated electrons in the doped AlSb transfer to InAs channel, we can estimate the carrier concentration in the AlSb(Te) layers. We did so for the samples of Fig. 3 as well as an additional sample with a doped Al_{0.6}Ga_{0.4}Sb layer. The results are plotted as down-triangles in Fig. 1. This data suggests that bulk Te-doping of AlSb may be limited to the mid 10^{18} cm^{-3} range. We note that two previous reports found that GaTe

doping of GaSb is limited to $1\text{--}2 \times 10^{18} \text{ cm}^{-3}$ [7,8]. A preliminary test of thick InAs(Te) on SI-GaAs, with $T_{\text{GaTe}} = 575^\circ\text{C}$ yielded $\sim 8 \times 10^{19} \text{ cm}^{-3}$ although the layer morphology was poor. If this result can be confirmed, higher densities might be achieved in InAs quantum wells by using a very thin InAs(Te) layer above the channel. An advantage over thin InAs(Si) layers [17] is that Te atoms that segregate or diffuse into the AlSb will still act as donors.

There has been concern about the use of Te doping in MBE systems because of the possibility of cross-talk between cells and contamination of the system resulting in high levels of Te background doping. We previously used Ga₂Te₃ and observed significant cross-talk problems. We have not observed cross-talk problems with GaTe. To check for background doping effects, we grew a 1.1 μm layer of GaAs doped with Te with $T_{\text{GaTe}} = 575^\circ\text{C}$. The carrier density was $1.3 \times 10^{19} \text{ cm}^{-3}$ as shown in Fig. 1. Immediately after this sample was grown, a 5 μm GaAs sample was grown with no intentional doping. The background doping was $p \sim 1 \times 10^{14} \text{ cm}^{-3}$, a typical value for this MBE before GaTe was introduced. We recently used GaTe in a new Riber 21 T MBE system. Despite the very different vacuum chamber and cell designs, the calibration curve is nearly identical to Fig. 1. This system also does not exhibit Te cross-talk or memory problems.

Chalcogens such as Te and Se have generally not been used in MBE for doping of arsenides because of potential surface segregation at high growth temperatures. In addition, Si has been shown to be a suitable dopant in most applications. With a limited number of cell ports on MBE machines, it could be useful if GaTe could be used to dope arsenides as well as antimonides. The data in Fig. 1 indicate that GaTe is a well-behaved dopant for GaAs, despite the fact that the growth temperatures were 550–600°C, higher than generally used for antimonide growth. The room-temperature mobilities for the GaAs(Te) samples in Fig. 1 were comparable to numbers obtained for GaAs(Si), e.g. 5000 cm²/Vs for the two samples at $4 \times 10^{16} \text{ cm}^{-3}$. As an additional test, we grew a sample consisting of 2.1 μm GaAs(Te)/1.1 μm undoped GaAs/GaAs-SI substrate. The GaTe cell

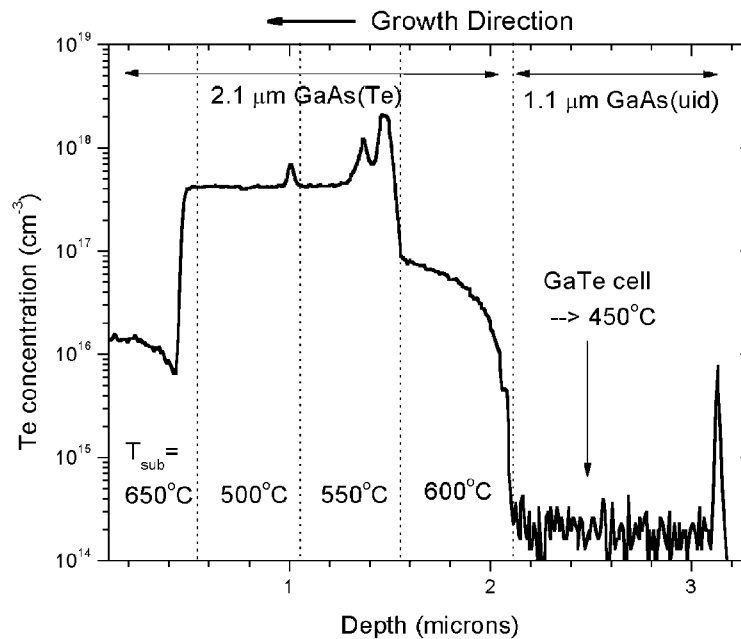


Fig. 4. SIMS profile of Te in GaAs with varying growth temperature. The growth direction is right to left with the substrate/epilayer interface at 3.1 μm .

temperature was brought up to 450°C during the growth of the undoped GaAs layer. As shown in the SIMS profile of Fig. 4, the Te background remained below the SIMS detection limit, indicating no significant leakage of GaTe around the shutter. Four different growth temperatures were used during the doped layer. The temperatures were measured by transmission thermometry [18]. For each change, the growth temperature was ramped over a period of 111 s without a growth interruption. The SIMS results indicate surface segregation of Te during growth at 600°C. When the temperature decreased to 550°C, the excess Te on the surface incorporated into the layer, yielding a doping spike of $2 \times 10^{18} \text{ cm}^{-3}$. The Te concentration then stabilized at $4 \times 10^{17} \text{ cm}^{-3}$. The next drop in temperature to 500°C resulted in a much smaller Te spike, followed by a return to the $4 \times 10^{17} \text{ cm}^{-3}$ levels. Finally, an increase in temperature to 650°C resulted in a large decrease in Te density, presumably due to surface segregation or desorption. Polaron profiling measurements on the same sample showed a carrier density

profile nearly identical to the SIMS profile of Fig. 4.

3. Conclusions

We used GaTe as an n-type dopant in several antimonide and arsenide III–V compounds. At a fixed GaTe flux, similar carrier densities were obtained in different host materials and at temperatures ranging from 350°C to 550°C. This temperature range encompasses the typical growth temperatures for antimonides and mixed arsenide/antimonide compounds. Alloys of InAlAsSb, needed for the emitter and collector in our 6.2-Å-lattice-constant HBT design, were successfully doped with GaTe at growth temperatures of 350–400°C. Although Te surface segregation is an issue for GaAs grown at 600–650°C, GaTe may be a suitable dopant for some GaAs- or InP-based applications. Carrier densities up to 10^{19} cm^{-3} were achieved in GaAs. Finally, no cell cross-talk

or memory problems were found with the use of GaTe in our MBE systems.

Acknowledgements

The authors thank J.B. Boos, E.R. Glaser, M. Goldenberg, K. Ikossi, and B.V. Shanabrook of NRL, R. Tsai of TRW, and G.W. Turner of Lincoln Laboratory for technical discussions and assistance and the Evans Analytical Group for SIMS measurements. The Defense Advanced Research Projects Agency supported this work.

References

- [1] B.V. Shanabrook, et al., SPIE Proc. 3790 (1999) 13.
- [2] R. Venkatasubramanian, D.L. Dorsey, K. Mahalingam, J. Crystal Growth 175 (1997) 224.
- [3] A. Furukawa, M. Mizuta, Electron. Lett. 24 (1988) 1378.
- [4] C.E.C. Wood, Appl. Phys. Lett. 33 (1978) 770.
- [5] S. Subbanna, G. Tuttle, H. Kroemer, J. Electron. Mater. 17 (1988) 297.
- [6] G.W. Turner, private communication.
- [7] K. Ikossi, M. Goldenberg, J. Mittereder, Solid State Electron. 46 (2002) 1627.
- [8] G.W. Turner, S.J. Eglash, A.J. Strauss, J. Vac. Sci. Technol. B 11 (1993) 864.
- [9] R. Magno, B.R. Bennett, K. Ikossi, M.G. Ancona, E.R. Glaser, N. Papanicolaou, J.B. Boos, B.V. Shanabrook, Proceedings of the 2002 Eastman Conference, IEEE, p. 288–296.
- [10] M. Kudo, T. Mishima, J. Crystal Growth 175 (1997) 844.
- [11] X. Li, Q. Du, J.B. Heroux, W.I. Wang, Solid State Electron. 41 (1997) 1853.
- [12] J.D. Werking, C.R. Bolognesi, L-D. Chang, C. Nguyen, E.L. Hu, H. Kroemer, Electron. Dev. Lett. 13 (1992) 164.
- [13] C. Nguyen, B. Brar, C.R. Bolognesi, J.J. Pekarik, H. Kroemer, J.H. English, J. Electron. Mater. 22 (1993) 255.
- [14] C.R. Bolognesi, E.J. Caine, H. Kroemer, IEEE Electron. Dev. Lett. 15 (1994) 16.
- [15] J.B. Boos, W. Kruppa, B.R. Bennett, D. Park, S. Kirchoefer, R. Bass, H.B. Dietrich, IEEE Trans. Electron. Dev. 45 (1998) 1869.
- [16] J.B. Boos, M.J. Yang, B.R. Bennett, D. Park, W. Kruppa, C.H. Yang, R. Bass, Electron. Lett. 34 (1998) 1525.
- [17] B.R. Bennett, M.J. Yang, B.V. Shanabrook, J.B. Boos, D. Park, Appl. Phys. Lett. 72 (1998) 1193.
- [18] B.V. Shanabrook, J.R. Waterman, J.L. Davis, R.J. Wagner, Appl. Phys. Lett. 61 (1992) 2338.